

A Method to Construct a Third-Generation Horseradish Peroxidase Biosensor: Self-Assembling Gold Nanoparticles to Three-Dimensional Sol–Gel Network

Jianbo Jia, Bingquan Wang,[†] Aiguo Wu, Guangjin Cheng, Zhuang Li, and Shaojun Dong*

State Key Laboratory of Electroanalytical Chemistry, Changchun Institute of Applied Chemistry, Chinese Academy of Sciences, Changchun, Jilin, 130022, P. R. China

A novel method for fabrication of horseradish peroxidase biosensor has been developed by self-assembling gold nanoparticles to a thiol-containing sol–gel network. A cleaned gold electrode was first immersed in a hydrolyzed (3-mercaptopropyl)-trimethoxysilane (MPS) sol–gel solution to assemble three-dimensional silica gel, and then gold nanoparticles were chemisorbed onto the thiol groups of the sol–gel network. Finally, horseradish peroxidase (HRP) was adsorbed onto the surface of the gold nanoparticles. The distribution of gold nanoparticles and HRP was examined by atomic force microscopy (AFM). The immobilized horseradish peroxidase exhibited direct electrochemical behavior toward the reduction of hydrogen peroxide. The performance and factors influencing the performance of the resulting biosensor were studied in detail. The resulting biosensor exhibited fast amperometric response (2.5 s) to H₂O₂. The detection limit of the biosensor was 2.0 $\mu\text{mol L}^{-1}$, and the linear range was from 5.0 $\mu\text{mol L}^{-1}$ to 10.0 mmol L⁻¹. Moreover, the studied biosensor exhibited high sensitivity, good reproducibility, and long-term stability.

In recent years, there has been considerable interest in applying immobilized enzymes to specific assays. Among these applications, the amperometric enzyme-based electrode is quite unique, because it combines the enzyme specificity with the sensitivity and convenience of electroanalytical techniques in a compact form to facilitate analysis.^{1–6} Much attention has been paid to the construction of the third generation biosensor, which is based on the direct electron transfer between the enzyme and the electrode.^{5,6} These studies developed an electrochemical basis

for the investigation of protein structure, mechanisms of redox transformations of protein molecules, and metabolic processes involving redox transformations. Until now, horseradish peroxidase (HRP) has been the commonly used enzyme for the construction of a third-generation biosensor.^{7–19} The enzyme contains heme as a prosthetic group, which is also the protein active site (with the resting state of the heme-iron: Fe(III)), and it can catalyze the hydrogen peroxide-dependent one-electron oxidation of a wide variety of substrates.²⁰

Molecular self-assembly has become a popular surface derivatization procedure, mostly owing to its simplicity, versatility, and the establishment of a high level of order on a molecular scale as a means of preparing modified surfaces.^{21–23} The high organization and homogeneity, together with its molecular dimension, make it very attractive for tailoring surfaces with desired properties. Many attempts have been made to fabricate a third-generation

- (7) Xiao, Y.; Ju, H. X.; Chen, H. Y. *Anal. Biochem.* **2000**, *278*, 22–28.
- (8) Zhao, J.; Henkens, R. W.; Stonehuerner, J.; O'Daly, J. P.; Crumbliss, A. L. *J. Electroanal. Chem.* **1992**, *327*, 109–119.
- (9) Zimmermann, H.; Lindgren, A.; Schuhmann, W.; Gorton, L. *Chem. Eur. J.* **2000**, *6*, 592–599.
- (10) Zhao, J.; Henkens, R. W.; Crumbliss, A. L. *Biotechnol. Prog.* **1996**, *12*, 703–708.
- (11) Chattopadhyay, K.; Mazumdar, S. *Bioelectrochemistry* **2001**, *53*, 17–24.
- (12) Chen, X.; Ruan, C.; Kong, J.; Deng, J. *Anal. Chim. Acta* **2000**, *412*, 89–98.
- (13) Ferri, T.; Poscia, A.; Santucci, R. *Bioelectrochem. Bioenerg.* **1998**, *45*, 221–226.
- (14) Ruzgas, T.; Gorton, L.; Emneus, J.; Marko-Varga, G. *J. Electroanal. Chem.* **1995**, *391*, 41–49.
- (15) Ho, W. O.; Athey, D.; McNeil, C. J.; Hager, H. J.; Evans, G. P.; Mullen, W. H. *J. Electroanal. Chem.* **1993**, *351*, 185–197.
- (16) Gorton, L.; Jonsson-Pettersson, G.; Csoregi, E.; Johansson, K.; Dominguez, E.; Marko-Varga, G. *Analyst* **1992**, *117*, 1235–1241.
- (17) Wollenbeger, U.; Wang, J.; Ozsoz, M.; Scheller, F. *Bioelectrochem. Bioenerg.* **1991**, *26*, 287–296.
- (18) Kulys, J. J.; Bililewski, U.; Schmid, R. D. *Bioelectrochem. Bioenerg.* **1991**, *26*, 276–286.
- (19) Yaropolov, A. I.; Malovik, V.; Varfolomeev, S. D.; Berezin, I. V. *Dokl. Akad. Nauk SSSR* **1979**, *249*, 1399–1401.
- (20) Hewson, W. D.; Hager, L. P. In *The Porphyrins*; Dolphin, D., Ed.; Academic Press: New York, 1979, Vol. VII B, Chapter 6.
- (21) Ulman, A. *An Introduction to Ultrathin Organic Films from Langmuir–Blodgett to Self-Assembly*; Academic Press: New York, 1991.
- (22) Swalen, J. D.; Allara, D. L.; Andrade, J. D.; Chandross, E. A.; Graeff, S.; Israelachvili, J.; McCarthy, T. J.; Murray, R.; Pease, R. F.; Rabolt, J. F.; Wynne, K. J.; Yu, H. *Langmuir* **1987**, *3*, 932–950.
- (23) Godinez, L. A. *Res. Soc. Quim. Mex.* **1999**, *43*, 219–229.

* Corresponding author. Fax: +86-431-5689-711. E-mail: dongsj@ns.ciac.jl.cn.

[†] Present address: DRFMC/SI3M/EMSI (UMR CNRS 5819), CEA de Grenoble, 17 Avenue des Martyrs, 38054 Grenoble, cedex 9, France.

- (1) Guo, L. H.; Hill, H. A. O. In *Advances in Inorganic Chemistry*; Sykes, A. G., Ed.; Academic Press: New York, 1991; Vol. 36, 341–375.
- (2) Ruzgas, T.; Csoregi, E.; Emneus, J.; Gorton, L.; Marko-Varga, G. *Anal. Chim. Acta* **1996**, *330*, 123–138.
- (3) Armstrong, F. A.; Wilson, G. S. *Electrochim. Acta* **2000**, *45*, 2623–2645.
- (4) Willner, I.; Katz, E. *Angew. Chem., Int. Ed.* **2000**, *39*, 1180–1218.
- (5) Ghindilis, A. L.; Atanasov, P.; Wilkins, E. *Electroanalysis* **1997**, *9*, 661–674.
- (6) Gorton, L.; Lindgren, A.; Larsson, T.; Munteanu, F. D.; Ruzgas, T.; Gazaryan, I. *Anal. Chim. Acta* **1999**, *400*, 91–108.

biosensor with self-assembly technology.^{7,9,24–26} For example, Chen et al.⁷ investigated the direct electron-transfer behavior of HRP immobilized on self-assembled gold colloid. Wink et al.²⁵ reviewed the biosensors based on self-assembled monolayers. However, all these works were based on planar self-assembly.

Sol–gel technology provides a unique means to prepare a three-dimensional network suited for the encapsulation of a variety of biomolecules.^{27–36} Sol–gel-derived inorganic materials are particularly attractive for biosensor fabrication, because they can be prepared under ambient conditions and they exhibit tunable porosity, high thermal stability, and chemical inertness, and they experience negligible swelling in aqueous solution. Our group has developed a new kind of sol–gel organic–inorganic hybrid material as a matrix for the fabrication of the biosensors.^{33,34} Lev et al.^{35,36} have developed bulk modified electrodes by physically encapsulating gold nanoparticles into porous sol–gel networks and exemplified their usefulness by demonstrating leak-free, reagentless biosensors for glucose. However, the above fabrication process of the second generation biosensor is complicated,³⁵ and the amount of enzyme needed for encapsulation is larger than that needed for self-assembly. To the best of our knowledge, no one has used a hydrolyzed three-dimensional sol–gel network to fabricate a self-assembled nanoparticle biosensor.

Recently, the opportunity to combine sol–gel and self-assembly technologies to prepare biosensor has emerged. Wang et al.³⁷ have used thiolated silicon alkoxides for designing, for the first time, a three-dimensional interfacial structure of silica gel on a gold electrode via the direct coupling of sol–gel and self-assembled technologies. The sol–gel of MPS develops a three-dimensional structure that is full of –SH.³⁸ Natan et al.^{39,40} have shown that gold nanoparticles are strongly bound to the surface through covalent bonds to the polymer functional groups, such as –CN, –NH₂, or –SH, and a gold nanoparticle monolayer can be prepared by self-assembly on the polymer-coated substrate. Therefore, gold nanoparticles can be assembled both inside the network and on the surface of the MPS sol–gel. This technology will exhibit the benefits of self-assembly, nanoparticles, and the increased surface area of three-dimensional electrodes. These

nanoparticles can act as tiny conduction centers and can facilitate the transfer of electrons.³⁸ The mechanism of electron transfer of gold nanoparticles has been widely investigated.^{36,38,41,42} For example, Willner et al.⁴² systematically studied the new electronic, photoelectronic, and sensor systems that are emerging from the functionalization of electrode surfaces with gold nanoparticle superstructures. What is more, biological macromolecules retain their activity when adsorbed on gold nanoparticles. Many works^{7,8,43–53} have shown that several enzymes maintain their enzymatic and electrochemical activity when immobilized on gold nanoparticles.

In this paper, we describe a new method to use a hydrolyzed three-dimensional sol–gel network to fabricate a self-assembled nanoparticle biosensor. At first, the MPS sol–gel containing –SH groups was self-assembled onto a gold electrode, then the gold nanoparticles were chemisorbed onto the –SH groups, and finally the HRP was adsorbed onto the surface of the gold nanoparticles. HRP was selected as a model, since it is well-studied and it is commercially available in a highly purified form. The biosensor fabrication procedure was optimized with respect to the size of the gold nanoparticles and the assembling time. In addition, the performance and factors influencing the performance of the resulting biosensor have been studied in detail.

EXPERIMENTAL DETAILS

Reagents. HRP (E.C. 1.11.1.7, type X, 250 units mg^{−1}) and MPS were obtained from Sigma. Chloroauric acid trihydrate (HAuCl₄·3H₂O) was purchased from EM Sciences. A 30% hydrogen peroxide solution was purchased from Beijing Chemical Reagent (Beijing, China), and a fresh solution of H₂O₂ was prepared daily. All other chemicals were of analytical grade and were used as received. Pure water was used throughout, which was obtained using a Millipore Q water purification set.

Apparatus. Amperometric and cyclic voltammetric experiments were performed using a Bioanalytical System BAS 100B/W (West Lafayette, IN). The temperatures of the solution in the electrochemical cell were adjusted by a superthermostat (Chongqing Experimental Instrument Factory, P. R. China). All experiments were carried out using a conventional three-electrode

(24) Mandler, D.; Turyan, I. *Electroanalysis* **1996**, *8*, 207–213.

(25) Wink, Th.; van Zuilen, S. J.; Bult, A.; Bennekom, W. P. *Analyst* **1997**, *122*, 43R–50R.

(26) Habermuller, K.; Mosbach, M.; Schuhmann, W. *Fresenius' J. Anal. Chem.* **2000**, *366*, 560–568.

(27) Walcarus, A. *Electroanalysis* **2001**, *13*, 701–718.

(28) Brinker, C. J.; Scherer, G. W. *Sol–Gel Science*; Academic Press: New York, 1990.

(29) Hench, L. L.; Valentine, J. K. *Chem. Rev.* **1990**, *90*, 33–72.

(30) Braun, S.; Rappoport, S.; Zusman, R.; Avnir, D.; Ottolenghi, M. *Mater. Lett.* **1990**, *10*, 1–5.

(31) Dave, B. C.; Dunn, B.; Valentine, J. S.; Zink, J. I. *Anal. Chem.* **1994**, *66*, 1120A–1127A.

(32) Li, J.; Tan, S. N.; Ge, H. *Anal. Chim. Acta* **1996**, *335*, 137–145.

(33) Wang, B.; Li, B.; Deng, Q.; Dong, S. *Anal. Chem.* **1998**, *70*, 3170–3174.

(34) Wang, B.; Li, B.; Wang, Z.; Xu, G.; Wang, Q.; Dong, S. *Anal. Chem.* **1999**, *71*, 1735–1739.

(35) Sampath, S.; Lev, O. *Adv. Mater.* **1997**, *9*, 410–413.

(36) Bharathi, S.; Lev, O. *Anal. Commun.* **1998**, *35*, 29–31.

(37) Wang, J.; Pamidi, P. V. A.; Zanette, D. R. *J. Am. Chem. Soc.* **1998**, *120*, 5852–5853.

(38) Bharathi, S.; Nogami, M.; Ikeda, S. *Langmuir* **2001**, *17*, 1–4.

(39) Freeman, R. G.; Grabar, K. C.; Allison, K. J.; Bright, R. M.; Davis, J. A.; Guthrie, A. P.; Hommer, M. B.; Jackson, M. A.; Smith, P. C.; Walter, D. G.; Natan, M. J. *Science* **1995**, *267*, 1629–1632.

(40) Grabar, K. C.; Freeman, R. G.; Hommer, M. B.; Natan, M. J. *Anal. Chem.* **1995**, *67*, 735–743.

(41) Hicks, J. F.; Zamborini, F. P.; Osisek, A. J.; Murray, R. W. *J. Am. Chem. Soc.* **2001**, *123*, 7048–7053.

(42) Shipway, A. N.; Lahav, M.; Willner, I. *Adv. Mater.* **2000**, *12*, 993–998.

(43) Patolsky, F.; Gabriel, T.; Willner, I. *J. Electroanal. Chem.* **1999**, *479*, 69–73.

(44) Crumbliss, A. L.; Perine, S. C.; Stonehuerner, J.; Tubergen, K. R.; Zhao, J.; O'Daly, J. P. *Biotechnol. Bioeng.* **1992**, *40*, 483–490.

(45) Crumbliss, A. L.; Perine, S. C.; Stonehuerner, J.; Tubergen, K. R.; Henkens, R. W.; Zhao, J.; O'Daly, J. P. *Proc. Conf. Trends Electrochem. Biosens.* **1992**, *43*–58.

(46) Crumbliss, A. L.; Stonehuerner, J.; Henkens, R. W.; Zhao, J.; O'Daly, J. P. *Biosens. Bioelectron.* **1993**, *8*, 331–337.

(47) Stonehuerner, J. G.; Zhao, J.; O'Daly, J. P.; Crumbliss, A. L.; Henkens, R. W. *Biosens. Bioelectron.* **1992**, *40*, 421–428.

(48) Henkens, R. W.; Zhao, J.; O'Daly, J. P. Peroxidase-colloidal gold-oxidase biosensors for mediatorless determination of glucose or other analyte. U.S. Patent 5225064, 1993.

(49) Crumbliss, A. L.; Stonehuerner, J. G.; O'Daly, J. P.; Zhao, J. *New J. Chem.* **1994**, *18*, 327–339.

(50) Zhao, J.; Stonehuerner, J.; O'Daly, J. P.; Henkens, R. W.; Crumbliss, A. L. *Biosens. Bioelectron.* **1996**, *11*, 493–502.

(51) Brown, K. R.; Fox, A. P.; Natan, M. J. *J. Am. Chem. Soc.* **1996**, *118*, 1154–1157.

(52) Yabuki, S.; Mizutani, F. *Electroanalysis* **1997**, *9*, 23–25.

(53) Xiao, Y.; Ju, H. X.; Chen, H. Y. *Anal. Chim. Acta* **1999**, *391*, 73–82.

system with the enzyme electrode as the working electrode, a platinum wire as the auxiliary electrode, and a Ag/AgCl (saturated KCl) electrode as the reference electrode. Cyclic voltammetric experiments were performed in quiescent solution. In steady-state amperometric experiments, the potential was set at -250 mV with a stirring rate of 300 rpm, and the current–time curves were recorded after a constant background current had been established. Electrolyte solutions were purged with high-purity nitrogen prior to and blanketed with nitrogen during electrochemical experiments. All of the electrochemical experiments were carried out in 5 mL of 50 mmol L⁻¹ phosphate buffer (PB, pH 7.0) at 20 °C by a thermostated water jacket unless otherwise stated.

Preparation of Gold Nanoparticles. All glassware used in the following procedures was cleaned in a bath of freshly prepared solution (3:1 HNO₃–HCl), thoroughly washed with water, and dried prior to use. The 20-nm-diam Au colloid was prepared according to the literature⁵¹ with a little modification. A solution of polydisperse 20-nm-diam Au colloidal particles was prepared by mixing 0.275 mL of 1% trisodium citrate and 0.750 mL of 0.075% NaBH₄/1% trisodium citrate with 100 mL of H₂O/0.500 mL 1% HAuCl₄ solution at room temperature, and stirring 5 h by a magnetic stirring bar at a stirring rate of 500 rpm. The Au colloids whose diameters were 41 and 71.5 nm were prepared according to Frens's method.⁵⁴ Briefly, 50 mL of 0.01% HAuCl₄ solution was heated to boiling, and 0.50 or 0.30 mL 1% trisodium citrate was added. The solution was kept boiling for 5 min. The particle sizes were confirmed by tunneling electron microscopy.

Preparation of Silica Sol. Silica sol was prepared by mixing MPS with water at a 1:4 ratio, 10% (v/v) of ethanol, and 3.3% (v/v) of 0.1 mol L⁻¹ hydrochloric acid;³³ the mixture was sonicated for 30 min until a clear and homogeneous solution resulted and was subsequently stored at room temperature for 2–3 h. Then the homogeneous and pellucid solution was used to self-assemble the gold electrode.

Preparation of the Biosensor. A bulk gold disk electrode was constructed using gold wire (99.99%, 1.0 mm diameter) in a soft glass tube, and it was polished carefully with 1.0-, 0.3-, and 0.05- μ m alumina slurry, and sonicated in water and absolute ethanol. Prior to the experiment, the bare gold electrode (BGE) was cyclic-potential scanned within the potential range of 1.5 to -0.3 V in freshly prepared deoxygenated 0.5 mol L⁻¹ H₂SO₄ until a voltammogram characteristic of the clean polycrystalline gold electrode was established.⁵⁵ The cleaned electrode was thoroughly rinsed with water and absolute ethanol and was immersed in the MPS sol–gel for 20 min at room temperature. The resulting self-assembled electrode was thoroughly rinsed with water to remove physically adsorbed silica sol. Then it was immersed in the gold nanoparticle solution for 10 h at 4 °C. Finally, the gold nanoparticle-modified electrode was incubated in 3 mg mL⁻¹ HRP (in 50 mmol L⁻¹, pH 7.0 PB) for 10 h at 4 °C to attach HRP molecules to the electrode surface. All resulting electrodes were washed with water and stored at 4 °C when not in use.

Atomic Force Microscopy (AFM). AFM measurements were performed using a digital Nanoscope IIIa multimode system (DI, Santa Barbara, CA). The images were acquired in the tapping mode. Measurements were made using the Si cantilever. The force

constant of the cantilever was 0.1–0.6 N/m with the scan rate at 1–2 Hz. The AFM measurements were made in air at room temperature. Gold substrates (10 \times 10 mm) were prepared by thermal evaporation of 5 nm Cr followed by 200 nm of Au onto silicon wafers that were precleaned by heating in piranha solution (7:3 mixture of concentrated sulfuric acid and 30% hydrogen peroxide) at 90 °C for 1 h. **Caution!** Piranha solution reacts violently with almost any organic materials and should be handled with extreme care! Prior to assembly, the gold substrates were treated with concentrated HNO₃ for 10 min, washed exhaustively with water and ethanol, and dried. Then the gold substrates were treated using the same procedures as for preparing the biosensor.

Measurement of HRP Activity on the Biosensor. The apparent activity of HRP immobilized on the biosensor was measured using the Trinder reaction.⁵⁶ H₂O₂ (1.7 mmol L⁻¹), 4-aminophenazone (2.5 mmol L⁻¹), and phenol (172 mmol L⁻¹) were mixed in a ratio of 2:1:1 in a microcuvette with a capacity of 2 mL. The prepared biosensor was inserted into the cuvette and agitated. After 3 min, the absorbance was measured at 510 nm, and the absorbance change per minute was calculated. An HRP calibration curve was obtained by repeating the above measurement using soluble enzyme. The amount of enzyme activity presented on the biosensor can be determined from the calibration curve.

RESULTS AND DISCUSSION

Scheme 1 gives the stepwise biosensor fabrication process. To monitor the formation of a self-assembled silica network on a gold substrate and examine the distribution of the gold nanoparticles and HRP, AFM was used to get the dynamic images after each assembly step. Figure 1 shows the AFM images of differently modified gold substrate. Figure 1a is the image of the surface of the bare gold substrate. As shown in Figure 1b, the hydrolyzed silicon alkoxide was assembled on the gold substrate surface and formed a network after the gold substrate was immersed in MPS sol–gel for 20 min. The surface roughness ranged from 4 to 7 nm, and there were some defects at the same time. Figure 1c reveals the broad distribution of gold nanoparticles after assembling the gold nanoparticles onto the substrate. The surface roughness is wavy from 5 to 27 nm. In view of the fact that the diameter of gold nanoparticles was 20 nm, gold nanoparticles should be both diffused into the sol–gel network and on the surface of it.³⁸ Such a distribution can provide a necessary conduction pathway and assist the electron transfer between the immobilized enzyme and the surface of the gold substrate. After the substrate was immersed in HRP solution for 10 h, the roughness was greatly reduced, and the surface became smooth, as evidenced by Figure 1d. (The mean roughness values for a, b, c, and d were 0.412, 0.901, 3.864 and 2.295 nm, respectively. See Supporting Information.) This result proves that HRP was successfully immobilized on the gold nanoparticles.

Cyclic voltammetry of ferricyanide is a valuable and convenient tool to monitor the barrier of the modified electrode, because the electron transfer between the solution species and the electrode must occur by tunneling either through the barrier or through the defects in the barrier. Therefore, it was chosen as a marker to investigate the changes of electrode behavior after each

(54) Frens, G. *Nature (Phys. Sci.)* **1973**, 241, 20–22.

(55) Sabatani, E.; Rubinstein, I. *J. Phys. Chem.* **1987**, 91, 6663–6669.

(56) Trinder, P. *Ann. Clin. Biochem.* **1969**, 6, 24–27.

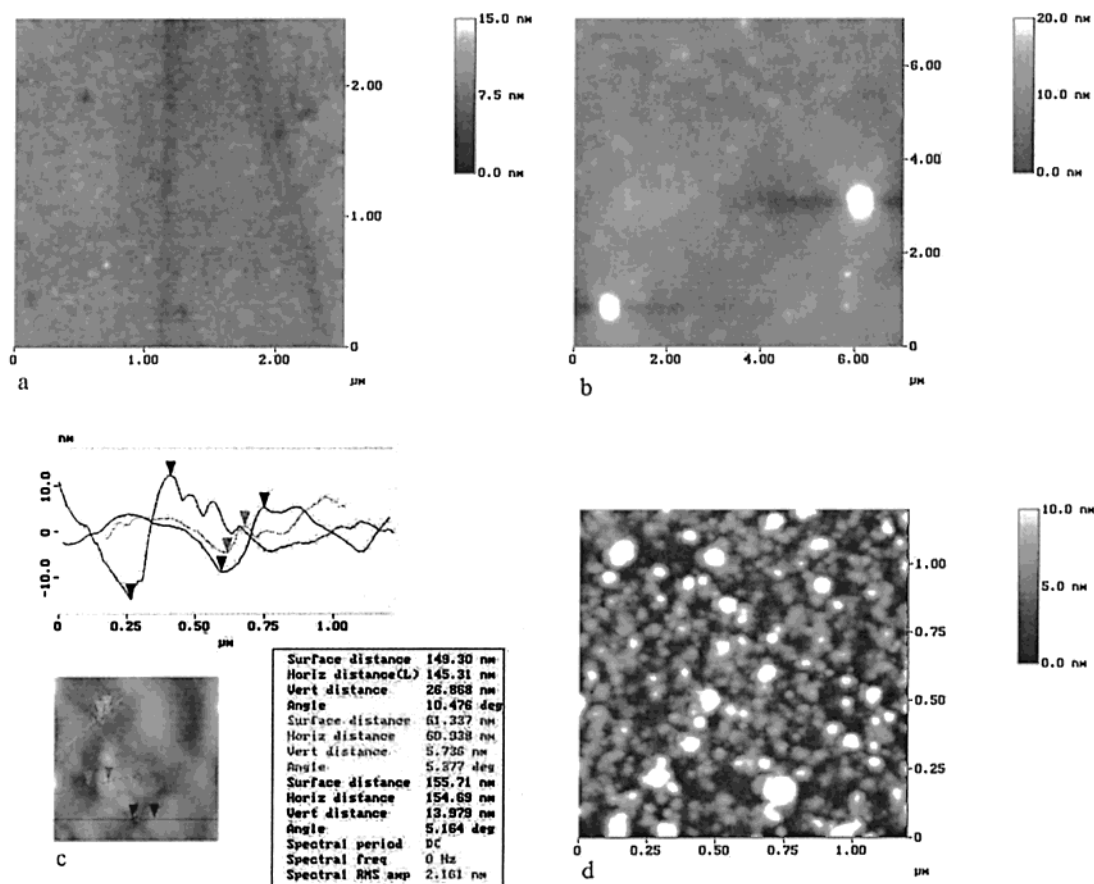
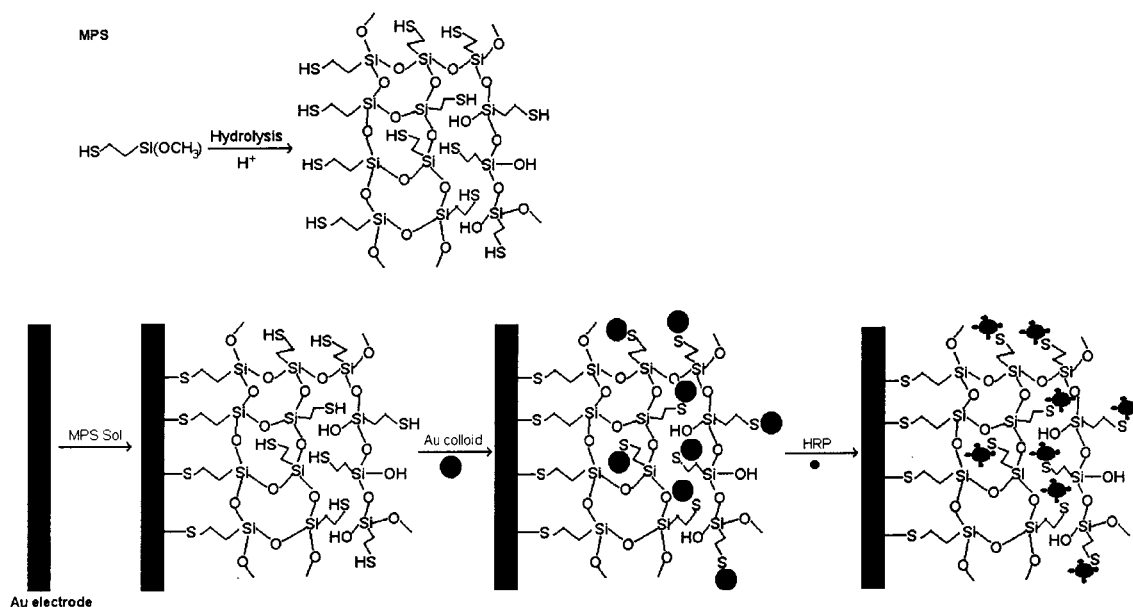


Figure 1. AFM images of differently modified gold substrates: a, the surface of the bare gold substrate; b, the self-assembled sol-gel on the gold surface; c, Au nanoparticles/sol-gel on the gold surface; and d, HRP/Au nanoparticles/sol-gel on the gold surface.

Scheme 1. Hydrolysis of MPS and the Stepwise Biosensor Fabrication Process



assembly step. Figure 2 shows cyclic voltammograms (CVs) of differently modified electrodes in 5.0 mmol L^{-1} ferricyanide solution. Well-defined CVs, characteristic of a diffusion-limited redox process, are observed at the bare gold electrode (Figure 2a). After dipping the electrode in the MPS sol-gel solution, an obvious decrease in the anodic peak and disappearance of the cathodic peak were observed (Figure 2b), which is in agreement

with previous results.^{37,38} The reason is that the silica sol-gel can act as the inert electron and mass transfer blocking layer, and it hinders the diffusion of ferricyanide toward the electrode surface. When gold nanoparticles were chemisorbed on the electrode, they were distributed throughout the sol-gel network and formed a continuous array of gold nanoparticles on the electrode. The remarkable current decreases in Figure 2c may be explained by

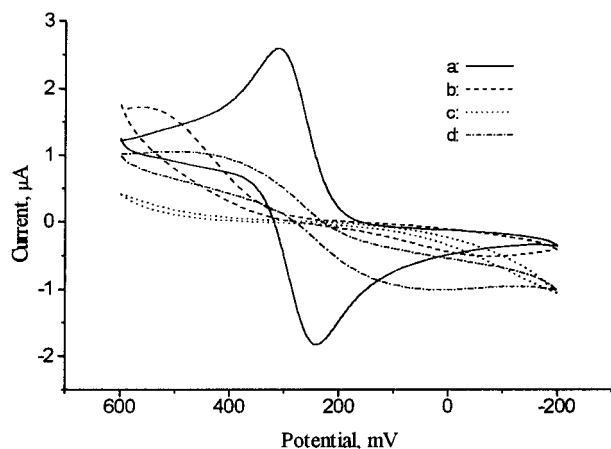


Figure 2. Cyclic voltammograms of the electrode at different stages: a, bare gold electrode (BGE); b, sol-gel/BGE; c, Au nanoparticles/sol-gel/BGE; d, HRP/Au nanoparticles/sol-gel/BGE. Supporting electrolyte, 5 mmol L⁻¹ Fe(CN)₆³⁻ + 0.1 mol L⁻¹ KCl; scan rate, 50 mV s⁻¹.

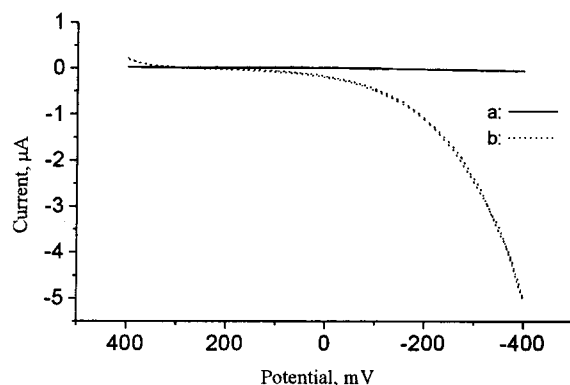


Figure 3. Cyclic voltammograms of HRP/Au nanoparticles/sol-gel/BGE in 50 mmol L⁻¹ pH 7.0 PB in the absence (a) and in the presence (b) of 2.5 mmol L⁻¹ H₂O₂. Scan rate, 10 mV s⁻¹.

the fact that the gold nanoparticles are a highly negatively charged species as a result of the adsorption of citrate in the fabrication process,⁵⁷ and they repulse the negatively charged ferricyanide. After HRP molecules were adsorbed onto the electrode surface, a quasireversible redox couple was observed (Figure 2d), but no redox peak could be observed in a 0.1 mol L⁻¹ KCl supporting electrolyte solution in the absence of ferricyanide. Therefore, the redox couple is due to the redox properties of ferricyanide. The isoelectric point of HRP is 8.9,⁵⁸ and it is positively charged in pH 7.0 PB solution. Therefore, the adsorbed HRP negates the effect of gold nanoparticles and increases the redox currents of ferricyanide. On the basis of the AFM and CV results, we can conclude that HRP is successfully immobilized on the self-assembled gold nanoparticles and we get the ideal structure of the biosensor (Scheme 1).

Figure 3 shows the CVs of the biosensor in 50 mmol L⁻¹ PB. In the absence of H₂O₂, no obvious current is found (Figure 3a), but a large catalytic current can be observed in the presence of 2.5 mmol L⁻¹ H₂O₂ (Figure 3b). To verify whether the current was due to nonenzymatic reduction of hydrogen peroxide, a control experiment in the absence of HRP was performed. Only

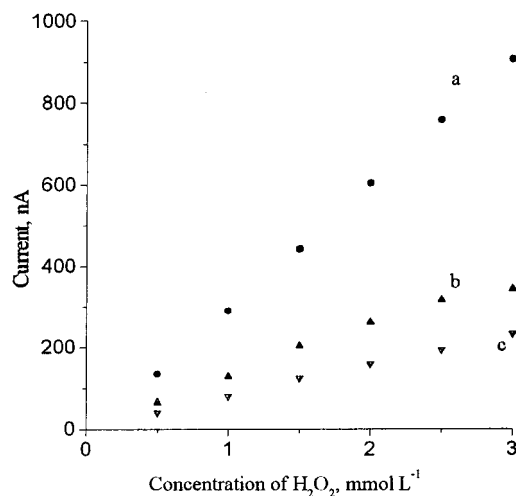


Figure 4. Steady-state amperometric responses of the biosensor with different sizes of gold nanoparticle to the reduction of H₂O₂ in the stirring PB: a, 20-nm gold nanoparticle; b, 41-nm gold nanoparticle; c, 71.5-nm gold nanoparticle. Applied potential, -250 mV; supporting electrolyte, 50 mmol L⁻¹ pH 7.0 PB.

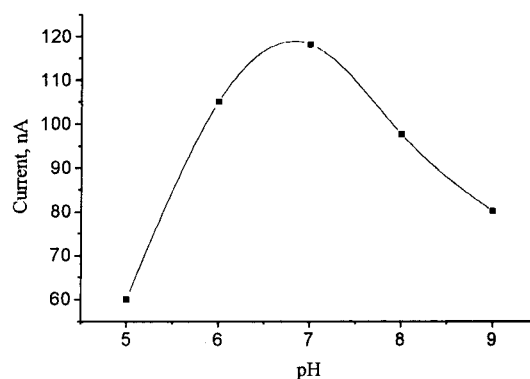


Figure 5. Effect of pH on the amperometric responses. Applied potential, -250 mV; supporting electrolyte, 50 mmol L⁻¹ PB; concentration of H₂O₂, 0.5 mmol L⁻¹.

a small current response to H₂O₂ can be observed at the Au nanoparticles/sol-gel/BGE electrode (see Figure 6). What is more, the response of the biosensor can nearly be eliminated in the presence of 25 mmol L⁻¹ S²⁻, which demonstrates that a catalytically active enzyme is an essential component of the biosensor. From these results, we confirmed that the catalytic current was mainly due to the direct electron transfer from the HRP molecules to the bulk electrode. Since gold nanoparticles are distributed both inside the sol-gel network and on the electrode surface, they allow efficient electron tunneling³⁸ and can assist the electron transfer between the redox protein and the bulk electrode surface.⁸

The effect of the size of the gold nanoparticles was studied, because it plays an important role in the biosensor performance. Figure 4 shows the amperometric responses of the biosensor with different sizes of gold nanoparticles to the reduction of H₂O₂ under steady-state condition. The magnitude of the steady-state current depends on the size of the Au colloid particles associated with the MPS sol-gel, which is in agreement with previous results.^{7,53} Doron et al.⁵⁹ reported that small-sized Au colloids could generate

(57) Weitz, D. A.; Lin, M. Y.; Sandroff, C. J. *Surf. Sci.* **1985**, *158*, 147–164.

(58) Weillinder, K. G. *Eur. J. Biochem.* **1979**, *96*, 483–502.

(59) Doron, A.; Katz, E.; Willner, I. *Langmuir* **1995**, *11*, 1313–1317.

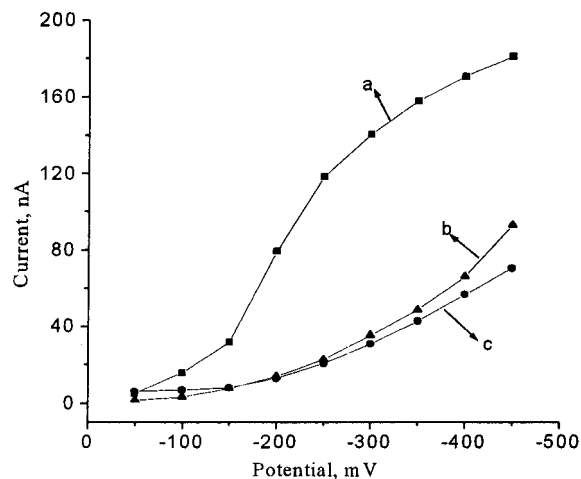


Figure 6. Effect of applied potential on the amperometric responses. a, HRP/Au nanoparticles/sol-gel/BGE; b, Au nanoparticles/sol-gel/BGE; c, HRP/sol-gel/BGE. Supporting electrolyte, 50 mmol L⁻¹ pH 7.0 PB; concentration of H₂O₂, 0.5 mmol L⁻¹.

continuous arrays of Au particles on the base monolayer, and the monolayer associated with the small-sized Au colloid film was more densely packed than the monolayer bound to the large-sized colloids. The pack of smaller-sized Au nanoparticle-bound MPS sol-gel is denser than that of the larger-sized Au colloids, providing more active binding sites for the immobilization of HRP. The biosensor fabricated with 20-nm gold nanoparticles exhibits a larger response than that of the other two sizes; therefore, 20-nm gold nanoparticles was chosen as the immobilized matrix.

The self-assembly time of the MPS sol-gel is the vital step for the fabrication of the biosensor. When the time was shorter, the amount of the self-assembled MPS sol-gel was little. It was not convenient to fabricate the biosensor at the following steps. When the time was longer, the response of the modified electrode to ferricyanide almost disappeared because of very strong adhesion features of the anchored sol-gel network, which seriously hinders the transfer of the electron. When a comparison was made of the electrodes being self-assembled in 10, 20, 30, 60, 90, and 120 min, respectively, 20 min was chosen as the proper self-assembled time.

The effect of pH on the biosensor behavior was studied between 4.0 and 9.0 in 50 mmol L⁻¹ PB. As shown in Figure 5, the current response increases from pH 4.0 to 7.0, and decreases from pH 7.0 to 9.0, which is in agreement with that reported for soluble HRP.⁶⁰ Thus, the gold nanoparticles matrix did not change the optimal pH value for the bioelectrocatalytic reaction of the immobilized HRP to H₂O₂.

The effect of applied potential on the steady-state current of the biosensor is shown in Figure 6. Electroreduction of H₂O₂ can be observed at -0.050 V, and the steady-state current increases as the applied potential shifts negatively from -0.050 to -0.500 V, which might be due to the increased driving force for the fast reduction of HRP at low potential. It is preferable to control the lower working potential to avoid or decrease the interference caused by some electroactive species at the electrode; therefore, -0.250 V was chosen as the working potential. The advantage of

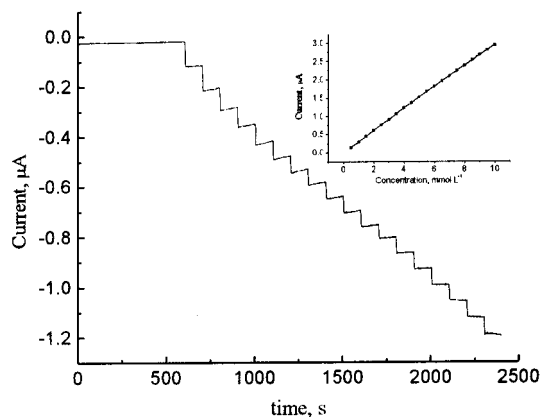


Figure 7. Typical steady-state response of the biosensor on successive injection of 0.5 mmol L⁻¹ H₂O₂ into 5 mL of stirring PB. Applied potential, -250 mV; supporting electrolyte, 50 mmol L⁻¹ pH 7.0 PB. Inset: the calibration curve of the biosensor.

using the gold nanoparticles can be seen from the comparison in Figure 6, in which the electrocatalytic current of H₂O₂ decreases significantly when no gold nanoparticles or HRP is available on the electrode. These results prove that gold nanoparticles play an important role in the biosensor response. Gold nanoparticles can act as a bridge to link thiolated sol-gel and HRP, and they can firmly immobilize HRP inside the sol-gel network. In addition, gold nanoparticles provide the necessary conduction pathways, and they can assist the direct electron transfer between the enzyme and the bulk electrode surface.

Figure 7 shows a typical current-time plot of the biosensor on successive addition of aliquot H₂O₂. As the H₂O₂ was added into the stirring buffer solution, the biosensor responded rapidly to the substrates. The biosensor could achieve 95% of the steady-state current within 2.5 s, which is faster than the previous reported result.⁸ Such a fast response can be attributed to two aspects: First, the HRP molecules are exposed to the surface of gold nanoparticles;⁷ therefore, H₂O₂ can diffuse to the enzyme freely. Second, gold nanoparticles are favorable to the orientation of the HRP molecule on the electrode in the process of bioelectrocatalysis, and they can transfer electrons more conveniently.⁸ The linear range of H₂O₂ is from 5.0 μmol L⁻¹ to 10.0 mmol L⁻¹ ($r = 0.997$; $n = 20$) with a detection limit of 2.0 μmol L⁻¹ estimated at a signal-to-noise ratio of 3. Spectrophotometric measurement of the soluble HRP activity showed the linear absorbance changes. The plot of absorbance change per min versus HRP activity is linear, with a slope of 7.51×10^{-3} . The activity of the HRP on the biosensor is 28.2 mU cm⁻². The sensitivity of the biosensor is 1282 nA dm³ μmol⁻¹ U⁻¹, which is higher than that of the electrodes used previously.^{15,61} Both gold nanoparticles⁴⁴ and organically modified sol-gel^{34,35} have little effect on enzyme activity, which may be the reason for the high sensitivity of the biosensor.

The thermal stability of the biosensor was studied in the presence of 0.5 mmol L⁻¹ H₂O₂ at different temperatures. Figure 8 shows that the current response increased with increasing temperature, reaching a maximum value at ~40 °C. This indicates that the activity of the immobilized enzyme increases as the

(60) Harbury, H. A. *J. Biol. Chem.* **1957**, *225*, 1009–1024.

(61) Deng, Q.; Dong, S. *J. Electroanal. Chem.* **1994**, *377*, 191–195.

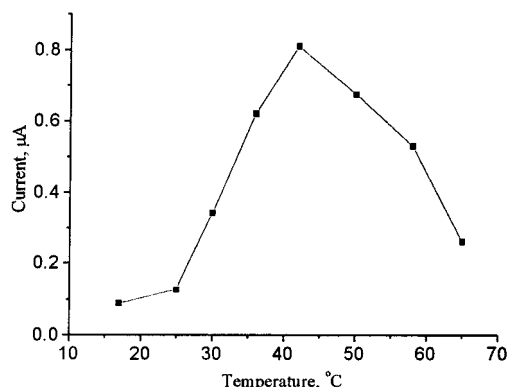


Figure 8. Effect of temperature on the amperometric responses. Concentration of H_2O_2 , 0.5 mmol L^{-1} ; applied potential, -250 mV ; supporting electrolyte, 50 mmol L^{-1} pH 7.0 PB.

temperature increases, but the enzyme may be partly denatured or desorbed from the gold nanoparticles when the temperature is too high.

The effect of substances that might interfere with the response of the biosensor was studied. The inhibition current obtained for each interfering substance presented at a concentration of 0.5 mmol L^{-1} (unless otherwise stated) was compared to that of $0.5 \text{ mmol L}^{-1} \text{H}_2\text{O}_2$, and this ratio was used as a criterion for the selectivity of the sensor. Similarly to a previous report,³⁴ glucose, sucrose, acetic acid, lactic acid, and ethanol did not cause any observable interference; only sulfide interfered significantly, and ascorbic acid and fluoride interfered slightly.

The repeatability and reproducibility of the biosensor were determined. The repeatability of one electrode to determine $0.5 \text{ mmol L}^{-1} \text{H}_2\text{O}_2$ was fairly good. The relative standard deviation (RSD) was 2.1% for 9 successive assays. The electrode-to-electrode reproducibility was estimated from the response to $0.5 \text{ mmol L}^{-1} \text{H}_2\text{O}_2$ at 6 different biosensors. This series yielded a mean current response of 124 nA and a RSD of 4.3%. Good reproducibility may be explained by the fact that the amount of self-assembled gold nanoparticles is consistent and HRP molecules are firmly attached on the surface of the gold nanoparticles.

The long-time stability of the biosensor was investigated over a 120-day period. When the biosensor was stored dry at 4°C and measured intermittently (every 2–3 days), no apparent change in the response to $1.0 \text{ mmol L}^{-1} \text{H}_2\text{O}_2$ was found over this period. However, when the gold nanoparticles were absent, the enzyme electrode retained only $\sim 50\%$ of its initial sensitivity to the reduction of $1.0 \text{ mmol L}^{-1} \text{H}_2\text{O}_2$ after two weeks. Good long-term

stability can be attributed to the strong interactions between the gold nanoparticles and HRP; therefore, HRP molecules can be firmly immobilized on the surface of the gold nanoparticles.

CONCLUSIONS

In this paper we have introduced a novel method for fabrication of a biosensor based on the combination of sol–gel and self-assembly technologies. The gold nanoparticles and HRP have been successfully immobilized on the electrode, and the direct electrochemistry of HRP has been shown. In addition, the biosensor that was studied exhibited fast response, good reproducibility, and long-term stability.

Several advantages of the proposed method should be highlighted. First, this approach is a universal immobilization method for biosensor fabrication. Thiol-containing silica gel can be assembled onto a gold electrode to form a three-dimensional network, which provides stereo attaching sites for gold nanoparticles. Because of the strong interactions between gold nanoparticles and biological macromolecules, enzymes and proteins can be firmly immobilized on the electrode. Glucose oxidase and urease have been successfully immobilized on the self-assembled electrodes, and these studies are under way. Second, it provides a general method to realize the direct electrochemistry of enzymes and proteins. Self-assembly of gold nanoparticles to silica gel provides the necessary conduction pathways and allows efficient electron tunneling, which makes it possible to realize direct electron transfer from the enzymes or proteins to the electrode surface. Third, gold nanoparticles can be assembled into a multilayer; thus, it can increase the enzyme loading. In addition, both gold nanoparticles and sol–gel have little effect on enzyme activity, and therefore, the resulting biosensor can have high sensitivity and good stability.

ACKNOWLEDGMENT

This work was supported by the National Natural Science Foundation of China (No. 29875028, 29835120). We thank Miss Z. Zhang and Mr. Z. Peng for the experimental help and discussion.

SUPPORTING INFORMATION AVAILABLE

The AFM images and roughness analysis of differently modified gold substrates. This material is available free of charge via the Internet at <http://pubs.acs.org>.

Received for review October 24, 2001. Accepted January 30, 2002.

AC011116W